Proceedings of the Institute of Acoustics

REFLECTION FROM MEDIA WITH CONTINUOUS VARIATION OF DENSITY, SOUND SPEED AND ATTENUATION

R C Chivers

Physics Department, University of Surrey, Guildford GU2 5XH

1 INTRODUCTION

The use of the simple model for the reflection of acoustic waves at a planar discontinuity of characteristic acoustic impedance is found in nearly all textbooks in acoustics although, regretfully, it is not usual to specify its assumptions. Specification of the assumptions, namely that it is valid for an infinitely extended plane wave normally incident on an infinitely extended infinitesimally thin planar interface between two infinitely extended homogeneous linear isotropic lossless media, reveals, that irrespective of its conceptual value, it is seldom realistic! Nevertheless it has significant achievements to its credit - not least as the basis of the development of diagnostic medical ultrasonics [1].

The practicality of the assumptions of infinite media and of planarity can be achieved to a reasonably high degree of approximation in practice by relation to the wavelength. Of greater importance, in many situations it is possible quantitatively to measure the degree of non-planarity and estimate its numerical significance. The introduction of anisotropy and regular inhomogeneity (whether in a deterministic or stochastic sense) will not be discussed in the present work. This will, rather, concentrate on the assumption of the Heaviside function change of characteristic impedance in the lossless case, and the subsequent introduction of losses in the form of attenuation. Specifically the reflection of plane waves from media whose acoustic properties vary as continuous functions of one dimension (depth) will be analysed. The lossless case is relatively straightforward and has appeared in different guises in several fields including geophysics and medical ultrasonics. The case which includes losses presents significant additional problems. An ad hoc procedure for dealing with these is suggested and an appropriate approximate analysis developed.

2 VARIATION OF CHARACTERISTIC ACOUSTIC IMPEDANCE

We can obtain a general understanding of the reflection processes involved in smoothly varying impedance changes from the following analysis. The particle displacement u(x,t) in a lossless medium obeys a wave equation of the form

$$\frac{1}{\rho(x)c^2(x)} \frac{\partial^2 u}{\partial t^2} = \frac{\partial}{\partial x}\left[\frac{1}{\rho(x)} \frac{\partial u}{\partial x}\right] \qquad (1)$$

where c(x) is the wave speed in the medium, $\rho(x)$ is its density and both are considered to be functions of distance x into the medium.

We assume a pressure impulse at x = 0, i.e.

$$\frac{\partial u}{\partial t}(0,t) = \delta(t) \qquad (2)$$

with the medium initially in equilibrium, i.e. $u(x,t) \equiv 0$ for $t < 0$.

REFLECTION FROM CONTINUOUS VARIATIONS

We further assume that the changes in density and sound speed are small so that the parameters at any value of x can be written as

$$c(x) = c_o + c_1(x) \quad \text{and} \quad \rho(x) = \rho_o + \rho_1(x) \tag{3}$$

The particle displacement is written in a similar way:

$$u(x,t) = u_o(x,t) + u_1(x,t) \tag{4}$$

where $u_1(x,t)$ is of the order of $c_1(x)$ and $\rho_1(x)$

Substituting these into equation (1) and collecting terms of the same order we obtain, for u_o:

$$\left.\begin{aligned} &\frac{1}{c_o^2}\frac{\partial^2 u_o}{\partial t^2} = \frac{\partial^2 u_o}{\partial x^2} \quad x > 0 \\ &\frac{\partial u_o}{\partial x}(0,t) = \delta(t) \\ &u_o(x,t) = 0 \quad \text{for } t < 0 \end{aligned}\right\} \tag{5}$$

and for $u_1(x,t)$:

$$\frac{1}{c_o^2}\frac{\partial^2 u_1}{\partial t^2} = \frac{\partial^2 u_1}{\partial x^2} + \frac{1}{c_o^2}\left(\frac{\rho_1}{\rho_o} + \frac{2c_1}{c_o}\right)\frac{\partial^2 u_o}{\partial t^2} - \frac{1}{\rho_o}\frac{\partial}{\partial x}\left[\rho_1 \frac{\partial u_o}{\partial x}\right] \tag{6}$$

$$\left.\begin{aligned} &\frac{\partial u_1}{\partial x}(0,t) = 0 \\ &u_1(x,t) = 0 \quad \text{for } t < 0 \end{aligned}\right\} \tag{7}$$

The solution for $u_o(x,t)$ is found to be a Heaviside function, H:

$$u_o(x,t) = - c_o\, H\left[t - \frac{x}{c_o}\right] \tag{8}$$

The solution for $u_1(x,t)$ is detailed elsewhere [2], and is best expressed in terms of the particle velocity:

$$\frac{\partial u_1}{\partial t}(0,t) = + c_1\left[x = \frac{c_o t}{2}\right] + \frac{c_o^2}{2\rho_o}\,\rho'\left[x = \frac{c_o t}{2}\right] \tag{9}$$

where the prime indicates differentiation. The overall impulse response in velocity is thus:

REFLECTION FROM CONTINUOUS VARIATIONS

$$\frac{\partial u}{\partial t}(0,t) = \frac{\partial u_0}{\partial t}(0,t) + \frac{\partial u_1}{\partial t}(0,t)$$

$$= -c_0\delta(t) + c_1'\left[x = \frac{c_0 t}{2}\right] + \frac{c_0^2}{2\rho_0}\rho'\left[x = \frac{c_0 t}{2}\right] \qquad (10)$$

Thus within the validity of the approximations used, the velocity impulse response at the surface of the medium at a time t is directly related to the gradients of the perturbations of the wave speed and the density at a distance to which the one-way travel time is t/2. Lizzi et al [3] found a similar result for the specific case of focussed transducer fields.

For situations in which ρ_1 and c_1 are not small quantities a numerical solution is advisable [4].

3 EFFECT OF LOSSES AT DISCONTINUITIES

If the boundary on which the plane wave is normally incident happens to be between two lossy media, of attenuation coefficients α_1 and α_2, the conventional formula for the amplitude reflection:

$$R = \frac{Z_2 - Z_1}{Z_2 + Z_1} \qquad (11)$$

becomes, instead [2]:

$$R = \frac{Z_2^2 - Z_1^2 + Z_2^2(\alpha_1/k_1)^2 - Z_1^2(\alpha_2/k_2)^2 - 2iZ_1Z_2(\alpha_1/k_1 - \alpha_2/k_2)}{(Z_1+Z_2)^2 + (Z_1\alpha_2/k_2 + Z_2\alpha_1/k_1)^2} \qquad (12)$$

where k_1 and k_2 are the wave numbers in the two media. It is interesting to note that if the attenuation coefficients depend linearly on the frequency, the reflection coefficient remains independent of frequency. It may be anticipated that the degree of extra complication entering the simple formula for the reflection at a discrete discontinuity, will be matched by a similar degree of increased complexity when continuous variations of attenuation are introduced.

4 CONTINUOUS VARIATION OF ATTENUATION

The introduction of continuous variations in the attenuation (in addition to those in sound speed and density) introduces a fundamental problem of analysis. The method adopted in section 3 was essentially a time domain approach with a delta function input. With the almost ubiquitous experimental evidence of the frequency dependence of the attenuation, this delta function will be distorted as it propagates into the medium, and to an extent that depends on the composition of the path traversed. It is not clear that a closed analytical solution to this problem is available.

In order to elucidate some of the physical mechanisms involved, an approach was adopted which appears at first sight to be non-physical, but which turns out to

REFLECTION FROM CONTINUOUS VARIATIONS

have direct physical application. It was assumed that the attenuation was independent of frequency, so that a delta function changes only in magnitude as a result of its propagation through the medium due to the changes in propagation parameters with depth, including the attenuation. The impulse response derived has physical meaning only in a remarkably limited number of situations.

However, in many practical situations, for example in underwater acoustics, the interrogating pulse is actually a tone-burst with a relatively narrow band of frequencies for which the attenuation is essentially single valued (but varying with depth). Thus provided the non-physical impulse response derived here is convolved with a tone-burst, the resulting echo train should be expected to give a very close approximation to the signals actually received.

As before, we look for a perturbational solution of the one-dimensional wave equation. The equation is:

$$\frac{1}{\rho c^2}\frac{\partial^2 u}{\partial t^2} + \alpha\frac{\partial u}{\partial t} = \frac{\partial}{\partial x}\left(\frac{1}{\rho}\frac{\partial u}{\partial x}\right) \tag{13}$$

where u is the particle displacement.

$$\text{Writing } \rho = \rho_0 + \rho_1(x),\quad c = c_0 + c_1(x),\ \alpha = \alpha_0 + \alpha_1(x) \quad \text{and } u = u_0 + u_1(x) \tag{14}$$

and substituting into equation (13) we obtain:

$$\frac{1}{\rho_0 c_0^2}\frac{\partial^2 u_0}{\partial t^2} + \alpha_0\frac{\partial u_0}{\partial t} = \frac{1}{\rho_0}\frac{\partial^2 u_0}{\partial x^2} \tag{15}$$

and

$$\frac{1}{\rho_0 c_0^2}\frac{\partial^2 u_1}{\partial t^2} + \alpha_0\frac{\partial u_1}{\partial t} - \frac{1}{\rho_0}\frac{\partial^2 u_1}{\partial x^2} = \dots$$

$$\dots = -\left(\alpha_1 + \rho_1\frac{\alpha_0}{\rho_0}\right)\frac{\partial u_0}{\partial t} - \frac{\rho_1^1}{\rho_0^2}\frac{\partial u_0}{\partial x} + \frac{2c_1}{\rho_0 c_0^3}\frac{\partial^2 u_0}{\partial t^2} \tag{16}$$

For a delta function input we have:

$$\frac{\partial u_0}{\partial t}(0,t) = \delta(t) \quad \text{and } u_0(x,t) = 0 \quad \text{for } t < 0 \tag{17}$$

Also

$$\frac{\partial u_1}{\partial x}(0,t) = 0 \quad u_1(x,t) = 0 \quad \text{for } t < 0 \text{ and for } c_0 t < x \tag{18}$$

REFLECTION FROM CONTINUOUS VARIATIONS

When $\alpha_o = 0$ the solution for u_o is the Heaviside function of equation 8. When $\alpha_o \neq 0$, a solution to equations (15) and (17) can be found [5] in the form:

$$u_o(x,t) = -\exp\left[-\frac{\beta x}{2}\right]H\left[t-\frac{x}{c_o}\right]-\frac{c_o^2}{2}\left[\frac{\beta}{2}\right]^2\exp\left[-\frac{\beta x}{2}\right]\left[t-\frac{x}{c_o}\right].H\left[t-\frac{x}{c_o}\right]+\ldots \tag{19}$$

where $\beta = \alpha_o c_o \rho_o$. From this we may obtain the particle velocity:

$$\frac{\partial u_o}{\partial t} = -\exp\left(-\frac{\beta x}{2}\right)\delta\left(t-\frac{x}{c_o}\right) - \frac{c_o^2}{2}\left(\frac{\beta}{2}\right)^2\exp\left(-\frac{\beta x}{2}\right)H\left(t-\frac{x}{c_o}\right)+\ldots \tag{20}$$

We may similarly obtain expressions for $\frac{\partial u_o}{\partial x}$ and $\frac{\partial^2 u_o}{\partial t^2}$ which can be inserted into equation (16).

After some analysis, the velocity "impulse response" is found in the form:

$$\frac{\partial u}{\partial t}(0,t) = -\delta(t) + \exp\frac{c_o^2\,\alpha_o\rho_o t}{2}\left\{\frac{c_o}{2}\left(\alpha_1(x)+\frac{\alpha_o\rho_1(x)}{\rho_o}\right)+\ldots\right.$$

$$\left.+\ldots\frac{\rho_1^1(x)}{2\rho_o}+\frac{c_1^1(x)}{c_o^2}\right\}\Bigg|_{x=\frac{c_o t}{2}} \tag{21}$$

The first term in this is generated by the half space surface. It is the structure of the remaining terms that is of particular interest. The last two terms of the last set of brackets are the terms obtained in the lossless case. The first two terms represent the effects due to the attenuation. The first of these is simply due to the spatial variation of the attenuation $\alpha_1(x)$. The second is the constant part of the attenuation weighted by the spatial variation of the density $\rho_1(x)/\rho_o$. The relation to the density derives from the form of the wave equation (equation (13)) used to define α. As may be expected, both the impedance and attenuation components are multiplied by the constant exponential decay of amplitude as the pulse propagates into the medium.

This exponential term will cause a general monotonic decay of the level of the reflected signal with time. The primary structure of the reflected signals is then seen to depend on the relative magnitudes of the effects due to the variations in the characteristic acoustic impedance and those due to attenuation variations. (This parallels directly the particular case of abrupt discontinuities in the parameters discussed briefly in section 3).

5 DISCUSSION

Notwithstanding the basic single-frequency assumption of this analysis it is only through the inclusion of attenuation that any frequency dependent effects can be interpreted since the analysis allowing variation of the sound speed and density of section 2 is essentially frequency independent.

REFLECTION FROM CONTINUOUS VARIATIONS

The use of echo-sounders for measuring the depth to the sea-bed is an excellent example of this, which fulfils the assumptions of the above analysis to a good degree of approximation. It is commonly observed that the depth recorded with an echo-sounder working at a given low frequency is greater than that operating at a higher frequency. Although there are more complex mechanisms involved in practice, the response obtained from a sea-bed that consists of a layer of silt or sand over the bedrock can be readily imagined. At low frequencies, the attenuation levels in the silt are low and its characteristic impedance is not too dissimilar from that of the water. After a small response between the silt and the water there will be a significant response as the silt becomes more compressed and particularly where it is bounded by the rock. This will be the most prominent response, which will be identified as that giving the depth of the sea-bed.

At high frequencies there will be significantly more attenuation in the silt. This will not only serve to reduce dramatically the size of the rock reflection (perhaps even below the noise level) but will also enhance the reflection from the water: silt interface. This latter, being the most prominent, will be regarded as that defining the depth of the sea-bed.

It can be seen that there are a number of future directions for valuable work. The use of the analysis presented for numerical calculations will be of practical value. The inversion of the problem would be of particular interest as would the extension of the analysis to situations involving greater changes in the parameters.

Acknowledgement

The author is grateful to Drs F Santosa and S Cornbleet for helpful discussions, to colleagues at Marine Microsystems and Irish Hydrodata in Cork for encouragement and to the EEC for support.

References

[1] P N T Wells (1977) Biomedical Ultrasonics, Academic Press, London

[2] R C Chivers and F Santosa (1986) Numerical considerations for interface reflections in medical ultrasound, Phys. Med. Biol. 31, 819-837

[3] F L Lizzi, M Greenebaum, E J Feleppa, M Elbaum and D J Coleman (1983), Theoretical framework for spectrum analysis in ultrasonic tissue characterization, J. Acoust. Soc. Am. 73, 1366-1373

[4] F Santosa and H Schwetlick (1982) The inversion of an acostical impedance profile by the method of characteristics, Wave Motion 4, 99-110

[5] F Santosa and R C Chivers, The one dimensional reflection problem in continuously varying lossy media, J. Acoust. Soc. Am. (submitted September 1987)

ULTRASONIC ABSORPTION MEASUREMENTS IN THIN FILMS OF ADHESIVE POLYMERS

R.E. Challis and T. Alper

University of Keele

Abstract

A novel wide bandwidth pulse transmission technique has been developed for the study of near plane wave ultrasound propagation in thin adhesive layers (down to 0.1 mm) set between aluminium or glass substrates. Acoustically thick PZT transducers in coaxial alignment are clamped on either side of the substrates; the transmitter is driven by very short voltage transients (120 V x 5 ns) and the receiver is terminated with a common base header amplifier. The signal received consists of a series of time resolvable multiple reverberations from the bond layer which are successively broader in the time domain due to the effects of absorption and velocity dispersion in the bond. The shapes of successive reverberations are compared in the frequency domain using conventional methods based on the FFT. Changes in the amplitude spectrum are used to calculate absorption as α, $\alpha\lambda$ or α/f^2 versus frequency in the range 1 MHz to 50 MHz. Calculations are also made of phase velocity versus frequency. Preliminary results for an epoxy adhesive at three stages of cure are presented.

Introduction

Adhesive bonding materials and associated fabrication techniques are at present in a stage of rapid development. In contrast, methods of evaluation of the mechanical properties of adhesives, and of testing bonds nondestructively, have not developed at the same rapid pace. This problem is particularly acute in the design of important structural components using adhered assemblies, such as automotive and aerospace body components, and high impact windscreens. Most methods of measurement of the bulk mechanical properties of adhesives are generally limited to large sample volumes and low driving frequencies and it is doubtful whether an adhesive polymer laid down as a thin film will have similar mechanical properties to those measured in a relatively large ingot of material. In addition to the mechanical properties of the bulk bond material, the adhesion properties between bond material and substrate are equally important in determining the engineering performance of an adhered structure. As far as the current authors are aware, there exists no reliable method of measurement of the mechanical properties of the adhesion boundary. The aims of this project have been to develop instrumentation in which

i) the viscoelastic properties of adhesive polymers in thin films (down to 0.1 mm) could be studied nondestructively in the frequency range 1 MHz to 50 MHz.

ii) the mechanical behaviour of the adhesive/substrate boundary subjected to small perturbations could be studied over the same frequency range.

A short pulse, wide bandwidth technique has been developed to achieve these aims and this paper reports the method, and our preliminary results for wave absorption in adhesives. The viscoelastic constants of the material will be obtained as estimates of the complex frequency dependent modulus governing wave propagation in the bond, derived from measures of wave absorption and phase velocity dispersion.

Measurement Technique

The layout of the bond test cell is shown in fig. 1. The adhesive material forms a bond between two aluminium or float glass substrates maintained with their faces parallel to within 0.05 degrees by cylindrical wire spacers. Acoustically thick (1) piezoelectric transducers (PZT, 10 mm diameter, 5 mm thick) are set in accurate coaxial allignment on either side of the test piece; one acts as transmitter and one as receiver. Transducer coupling is achieved by a thin layer of compressed aluminium foil (0.015 mm) that also acts as an electromagnetic screen between transmission and reception circuits. Short high voltage pulses (160 V by 1.5 ns, adjustable to 20 ns) are generated in an avalanche transistor generator circuit and these are applied to the transmitting transducer. The receiving transducer is connected to a header amplifier of 150 MHz bandwidth and the output of this is digitised either at 200 MHz using a Le Croy TR8828 transient recorder, or at 1 GHz by means of a sampling oscilloscope feeding a conventional successive approximation analogue to digital converter operating at 50 KHz. Digitised signals are processed on a network of PDP11 series minicomputers.

When the transmitting transducer is excited a bounded plane-wave near-relica of the exciting waveform leaves the transducer front face and enters the glass substrate (a) of the test cell. It propagates to the adhesive layer and sets up a short sequence of acoustic reverberations in the adhesive material. Part of this sequence propagates across the second glass substrate (b) to the receiving transducer. This first disturbance to reach the receiver is followed by a complex set of reverberations that are excited in both of the glass substrates, both of the transducers, and the structure of the rig supporting the cell and transducers. The thickness of the transducers and of the glass plates is chosen to give acoustic reverberation times in those components that are very much greater than the expected reverberation times in the adhesive layer. This enables the first reverberation complex from the bond to be extracted from all of the other received disturbances by a time domain window applied to the digitised waveforms. Successive reverberations in this extracted complex are separately identifiable in the time domain (fig. 2), and become increasingly broader and flatter as the number of transits of the adhesive layer increases. Frequency domain measures of the change in shape between successive reverberations are used to extract absorption and phase velocity in the adhesive as functions of frequency.

Formation of the Reverberation Signal

In the analysis that follows the Laplace transform notation is used for electrical and acoustic signal variables. Convolution operations that describe the effect of the physical elements of the system on the signal pathway are therefore interpreted as multiplications between Laplace transforms of signals and appropriate element responses to Dirac function ($\delta(t)$) excitation. We identify a Laplace domain transfer function for each element in the signal pathway shown on fig. 1.

Transmitter transducer	$G_1(s)$
Transmitter transducer coupling	$G_2(s)$
Glass block (a)	$G_3(s)$
Adhesive layer	$T_{123}(s)$
Glass block (b)	$G_4(s)$
Receiver transducer coupling	$G_5(s)$
Receiver transducer	$G_6(s)$
Transient diffraction	$G_7(s)$

The overall transfer function for the signal pathway is

$$F(s) = G_1(s)G_2(s)G_3(s)G_4(s)G_5(s)G_6(s)G_7(s)T_{123}(s) \qquad (1)$$

All of the non adhesive parts of the system can be lumped into a single function $G(s)$, and $T_{123}(s)$ can be obtained by solution of the one dimensional wave equation in the adhesive layer, assumed for the present to be homogeneous and isotropic.

$$T_{123}(s) = \frac{T_{12}(s)\, T_{23}(s)\, H(s)\, e^{-s\tau}}{1 - R_{21}(s)R_{23}(s)H^2(s)e^{-2s\tau}} \qquad (2)$$

Refering to fig. 1, $T_{12}(s)$ and $T_{23}(s)$ are the pressure transmission coefficients through the 1-2 and 2-3 boundaries, $R_{21}(s)$ and $R_{23}(s)$ are the internal pressure reflection coefficients for waves within the bond region reflected internally at its boundaries, and $H(s)$ describes the frequency filtering effect of absorption during a single transit of the adhesive layer. The exponential terms represent the time delay for a single transit across the bond. Expanding the denominator of eq. 2 by the binomial theorem and including the fixed system effects, G(s) we obtain the following description of the signal pathway in the gated time interval.

$$F(s) = G(s)T_{12}(s)T_{23}(s)H(s)e^{-sT}\,[1 + A(s) + A^2(s) + \ldots\ldots A^n(s)\ldots\ldots]$$

$$\text{Where } A(s) = e^{-2sT}\,R_{21}(s)R_{23}(s)H^2(s) \qquad (3)$$

The three discrete reverberations shown in fig. 2 can be associated with terms in the series of eq. 3. Identifying the pulses as $A_1(s)$, $A_2(s)$ and $A_3(s)$, and lumping the terms outside of the square bracket as B(s) we get

$$A_1(s) = B(s)$$

$$A_2(s) = B(s)\,A(s)$$

$$A_3(s) = B(s)\,A^2(s) \qquad (4)$$

B(s) can be eliminated by forming the quotient of any pair of equalities in equs. 4. This yields,

$$A(s) = A_2(s)/A_1(s)$$

$$\text{or} \quad A(s) = A_3(s)/A_2(s) \qquad (5)$$

Thus by appropriate computer manipulations of the measured successive reverberations A_1, A_2, A_3 it is possible to estimate the frequency filtering effect of a single transit across the adhesive layer, combined with the two internal reflections R_{21} and R_{23}. With repeated experiments on bonds of different thickness but otherwise identical formation it is also possible to separately characterise propagation in the bulk adhesive, H(s) and the double internal reflection processes ($R_{21}(s)\,R_{23}(s)$).

Computations

We recall that A(s) contains a time delay term e^{-sT} that represents a to-fro pair of pulse transits across the adhesive layer. The computational procedure required to extract A(s) from digitised bond reverberation signals must therefore first remove this time shift before estimating the quotients A_2/A_1 or A_3/A_2. The procedure is as follows:

i) Apply a rectangular window with a 10% cosine taper at each end to each of the time resolvable reverberations A_1 A_2 A_3. This is done interactively using a screen graphics facility.

ii) Align A_1 A_2 and A_3 in the time domain, first approximately. Using interactive procedures and then more precisely by estimating a few lags of the time domain cross correlation functions between the pairs A_1A_2 and A_2A_3 and shifting each complex with respect to its partner to maximise correlation.

iii) Pad the resulting aligned complexes with zeros up to an integer power of 2 points (generally 512) in preparation for fast Fourier transformation. (FFT).

iv) Apply a circular shift in order to set the peak value of each complex at the beginning of its data array. This maximises the real component of the FFT output, in relation to the imaginary component.

v) Calculate the FFT of each zero-padded, shifted complex.

vi) Form the quotients of the FFTs to give estimates of A_2/A_1 and A_3/A_2. In this procedure we protect against excessive variance in the results by forming up to 256 averages of successive recordings of the time domain signal before computation, and then by ignoring spectral components whose modulus is a factor k less than the maximum value in each data set. Working values of k range from 10 to 200.

v) Calculate the modulus and phase spectrum of each quotient.

vi) Calculate the apparent absorption coefficient for the adhesive material as a function of frequency thus,

$$\alpha(f) = [\ln (A_2/A_1)]/x \qquad (6)$$

where x is the to-fro path length in the adhesive and f is frequency. At present this procedure neglects any frequency dependence in the internal reflection coefficients R_{21} R_{23}, see the following section.

vii) Estimate the phase velocity from the phase spectrum difference data on the basis of phase lag due to propagation over distance x given by

$$\theta(x,f) = - j2\pi fx/c(f) \qquad (7)$$

where c(f) is phase velocity

viii) Calculate absorption per wavelength $\alpha\lambda$, or α/f^2 as functions of frequency.

ix) Although our method is not fully developed at this stage, we have made estimates of the complex modulus governing near plane wave propagation in adhesive polymers on the basis of our absorption and velocity dispersion results. These will be the subject of a future communication.

Preliminary Results

Absorption and velocity dispersion measurements have been made on a number of adhesive polymers using the method described above. An example of $\alpha\lambda$ versus frequency and c(f) versus frequency for an epoxy adhesive at three stages of cure is shown in fig. 3. The solid lines on fig. 3a show approximate fits of single relaxation processes to the measured data; the measured data are shown as discrete points. The solid lines on the phase velocity curves (fig 3b) are predictions of phase velocity on the basis of the fitted relaxation processes, and again the measured values are indicated as discrete points.

Discussion

The results so far indicate that measurements of absorption and velocity dispersion over reasonably wide frequency bandwidths are possible for adhesive polymers in thin films, down to 0.1 mm. We have not yet formally separated the estimation of $R_{21}(s)$ and $R_{23}(s)$ from the estimation of H(s).

The signal to noise ratio of the measurement technique is at present lower than we intend, due to the difficulties of maintaining wide signal bandwidths in hybrid analogue and digital instrumentation where the insertion loss in the signal pathway is high. This problem is compounded by the limited resolution of fast digitising hardware, at present of the order of eight binary bits. Future work will concentrate on four areas:

i) The improvement of the signal to noise conditions in the apparatus

ii) The design of software modules to reduce the interactive nature of the computations.

iii) The automatic extraction of real and imaginary parts of the elastic modulus governing wave propagation in the adhesive.

iv) Study of wave propagation at the interfaces between adhesive and substrate by estimation of the internal reflection coefficients R_{21} and R_{23}

References

1. R.G. Peterson and M. Rosen, J. Acoust. Soc. Am., 41, 336-341, 1966.

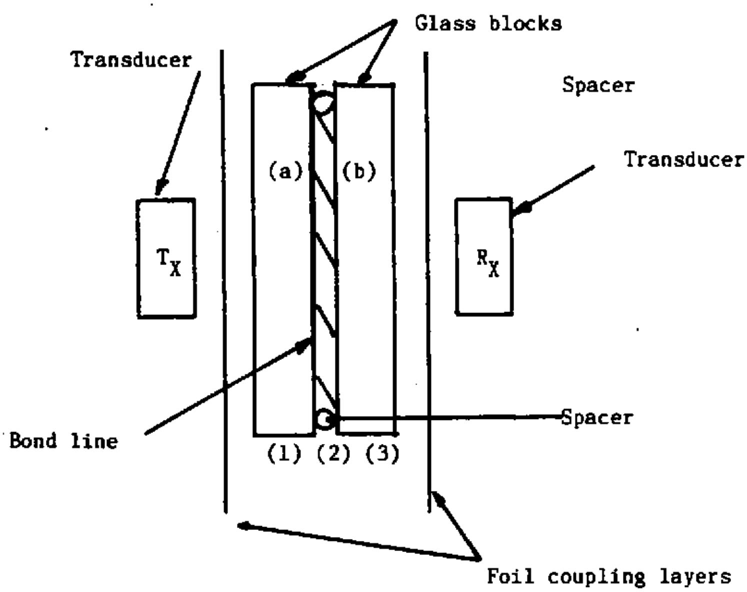

Fig. 1 Diagram illustrating the principal elements of the experimental apparatus. The elements are shown expanded out with spaces between them for clarity of presentation. In practice they are squeezed together in a clamp.

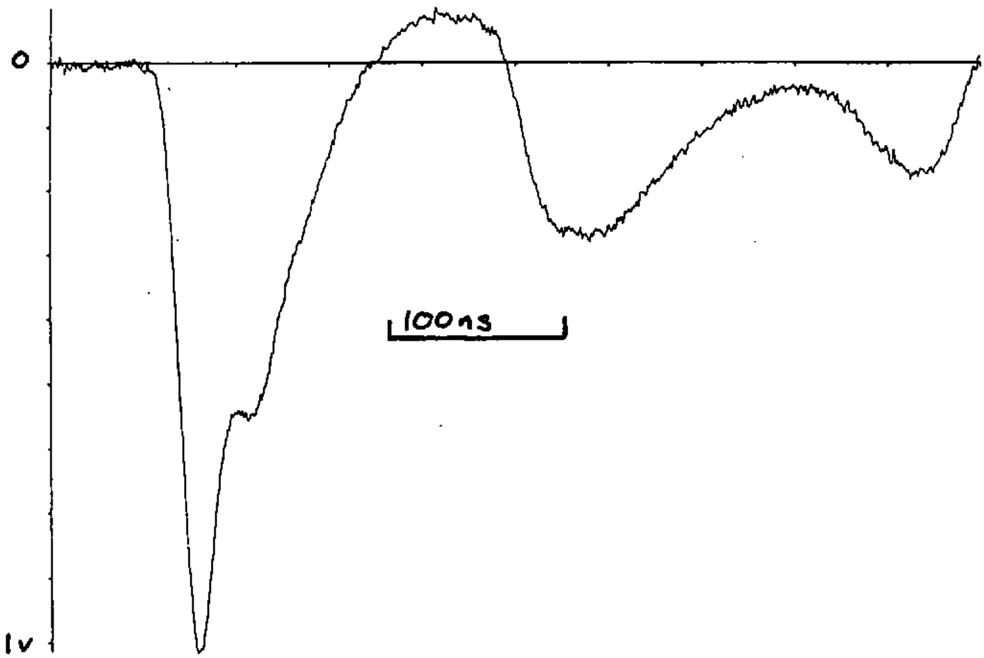

Fig. 2 Time domain record of three successive reverberations in a test bond.

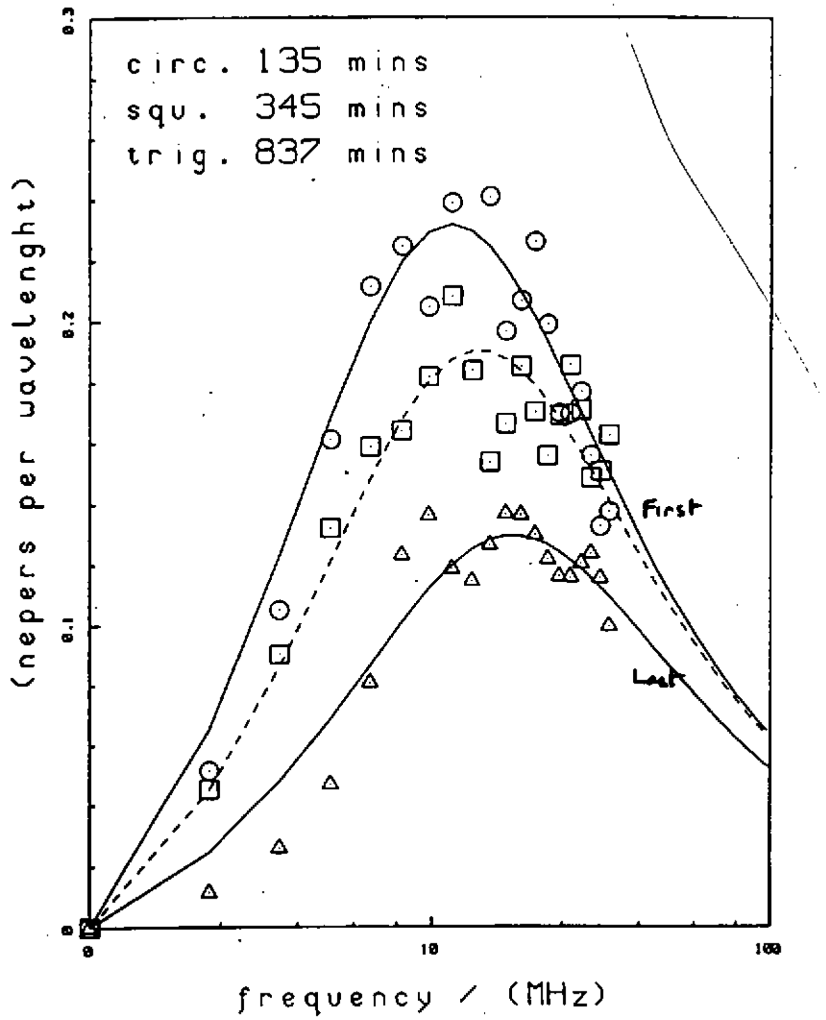

Fig. 3 a) αλ for an epoxy adhesive at three stages during cure

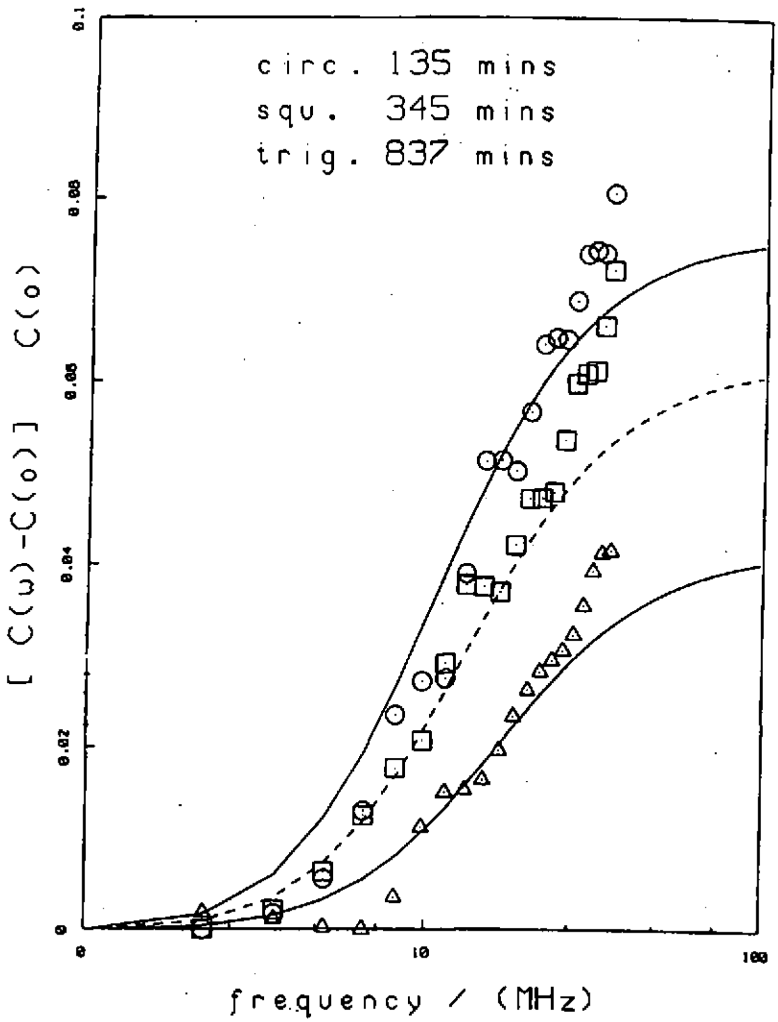

Fig 3 b) c(f) for the same bond, again at three stages of cure